International Journal of Hyperthermia

ISSN: 0265-6736 (Print) 1464-5157 (Online) Journal homepage: www.tandfonline.com/journals/ihyt20

High intensity focused ultrasound: Physical principles and devices

Dr >Gail ter Haar & Constantin Coussios

To cite this article: Dr >Gail ter Haar & Constantin Coussios (2007) High intensity focused ultrasound: Physical principles and devices, International Journal of Hyperthermia, 23:2, 89-104, DOI: 10.1080/02656730601186138

To link to this article: https://doi.org/10.1080/02656730601186138

Int. J. Hyperthermia, March 2007; 23(2): 89–104

informa
healthcare

High intensity focused ultrasound: Physical principles and devices

GAIL TER HAAR[1], & CONSTANTIN COUSSIOS[2]

[1]*Joint Physics Department, Institute of Cancer Research: Royal Marsden NHS Foundation Trust, Sutton, Surrey, SM2 5PT, UK and* [2]*Deptartment of Engineering Science, Institute of Biomedical Engineering, University of Oxford, Oxford OX1 3PJ, UK*

(Received 22 December 2006; accepted 24 December 2006)

Abstract
High intensity focused ultrasound (HIFU) is gaining rapid clinical acceptance as a treatment modality enabling non-invasive tissue heating and ablation for numerous applications. HIFU treatments are usually carried out in a single session, often as a day case procedure, with the patient either fully conscious, lightly sedated or under light general anaesthesia. A major advantage of HIFU over other thermal ablation techniques is that there is no necessity for the transcutaneous insertion of probes into the target tissue. The high powered focused beams employed are generated from sources placed either outside the body (for treatment of tumours of the liver, kidney, breast, uterus, pancreas and bone) or in the rectum (for treatment of the prostate), and are designed to enable rapid heating of a target tissue volume, while leaving tissue in the ultrasound propagation path relatively unaffected. Given the wide-ranging applicability of HIFU, numerous extra-corporeal, transrectal and interstitial devices have been designed to optimise application-specific treatment delivery. Their principle of operation is described here, alongside an overview of the physical mechanisms governing HIFU propagation and HIFU-induced heating. Present methods of characterising HIFU fields and of quantifying HIFU exposure and its associated effects are also addressed.

Keywords: *Ultrasound therapy, thermal ablation, cancer, heating, high intensity focused ultrasound (HIFU)*

Introduction

The aim of most ablative therapies, whether for the treatment of cancer or of benign conditions, is the selective destruction of a targeted tissue volume, leaving surrounding tissues intact. The intention of a high intensity focused ultrasound (HIFU) treatment is to raise the temperature of a selected, isolated tissue volume above 55°C and to maintain this temperature for 1 s or longer. It is known that 55°C held for this time will lead to coagulative necrosis and immediate cell death [1, 2]. In theory, this is possible with a focused ultrasound beam since the short (mm) wavelengths of ultrasound at megaHertz frequencies in soft tissue allows it to be focused into small, clinically relevant, volumes. Ultrasonic energy absorption within the focal volume induces high temperatures locally at the focus, with temperatures outside this region being kept at levels that are not cytotoxic. The volume of destroyed cells is referred to as a ''lesion''. The principle of HIFU is shown in Figure 1. An important feature of HIFU lesions is that the damage is spatially confined with no surrounding cellular damage. They are often referred to as ''trackless''. In this sense they are different from those produced by other ablative therapies which necessitate the introduction of an applicator into the target volume [3–14]. The cross-sectional histological appearance of HIFU lesions in liver, prostate and brain has been referred to as an ''island and moat'' structure [15]. Thermal damage produced by a heated wire has a similar appearance [15, 16]. In the liver, the margin of the lesion has been shown, 2 h after exposure, to consist of a rim of glycogen free cells ~10 cells wide [17]. These cells, which otherwise appear normal, are dead 48 h later. Cells

Correspondence: Dr Gail ter Haar, Joint Department of Physics, Royal Marsden NHS Foundation Trust, Downs Road, Sutton, Surrey, SM2 5PTUK. Tel: +44-208-661-3703. Fax: +44-208-643-3812. E-mail: gail.terhaar@icr.ac.uk

ISSN 0265–6736 print/ISSN 1464–5157 online
DOI: 10.1080/02656730601186138

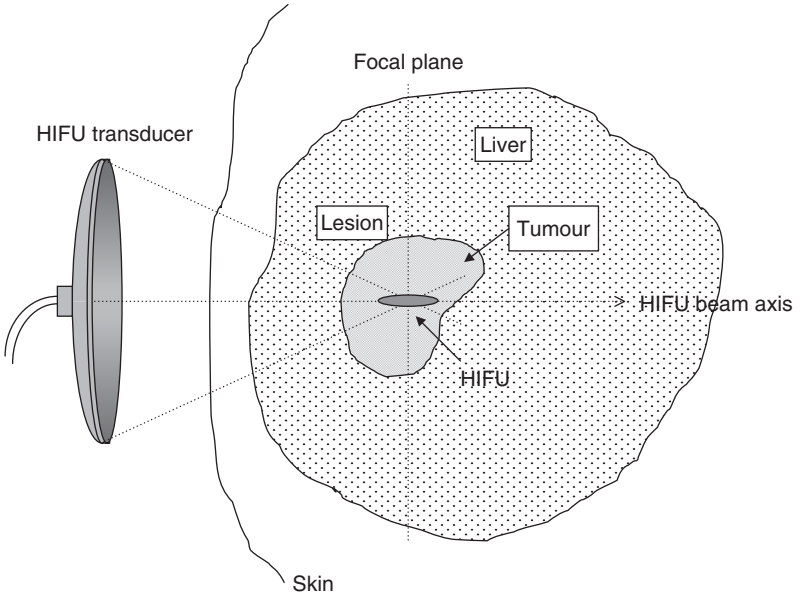

Figure 1. Diagrammatic illustration of the principle of HIFU. High-intensity ultrasound waves are generated by a transducer outside the body and focussed onto a small region deep within tissue. HIFU-induced heating causes cell death by thermal necrosis within the focal volume, but leaves tissue elsewhere in the propagation path unaffected.

within the island exhibit coagulative necrosis typical of thermal injury. A key objective of a HIFU treatment is to delivery the energy required to raise the tissue temperature to a cytotoxic level sufficiently fast that the tissue vasculature does not have a significant effect on the extent of cell killing, that is, that cooling due to blood perfusion or heat diffusion is not important. It has been shown that HIFU can lead to vessel wall disruption and also to vascular occlusion [17–28].

The clinical applications for HIFU that have been widely explored lie in neurosurgery, ophthalmology, urology, gynaecology and oncology.

History

The first suggestion that high intensity ultrasound beams might be used for therapeutic purposes came in 1942 [29], but the first report of application of HIFU to humans was not until 1960 [30, 31]. This technique did not gain significant clinical acceptance until the 1990s, despite successful ophthalmological treatments before this date. Early equipment was heavy and unwieldy, and the original applications proposed were in the brain, which involved surgical intervention to remove bone. The development of HIFU coincided with the introduction of the drug L-dopa. From a patient's perspective, L-dopa proved to be a more acceptable treatment for Parkinson's disease. The lack of imaging sophistication also restricted the growth of HIFU applications at that time. In order to capitalise on the precision of the cell killing proffered by HIFU, it is necessary to be able to achieve accurate placement of ''lesions'' within the target volume. Precise targeting and good treatment follow-up techniques (with anatomical and functional imaging), are only now available with diagnostic ultrasound scanning and magnetic resonance imaging (MRI) techniques, thus paving the way to realising the full potential of HIFU treatments.

Early attempts to place ultrasound lesions in the brain through the intact skull bone were unsuccessful [29, 32]. Small lesions were found in the brain, but there was profound damage to the scalp. Mode conversion and the high acoustic absorption of bone lead to a high degree of attenuation in the skull bone. Only once a window had been made in the skull, could discrete lesions be placed deep within the brain [33–36]. White matter appears to be more susceptible to damage than grey matter [36, 37]. Fifty patients with Parkinson's disease were amongst the first people to be treated with HIFU [31]. Following craniotomy, the *Substantia negra* and *Ansa lenticularis* were exposed through the dura under local anaesthetic. The procedure took 14 h. Although it was claimed that the symptoms of Parkinsonism were eliminated, this treatment does not appear to have been taken further, probably because of the concurrent development of the drug L-dopa mentioned above. The requirement to remove a section of skull bone, combined with targeting complexity limited the progress of this neurosurgical research. However, phase correction (time reversal) techniques may allow the focus to be reconstructed

following transmission through bone [38, 39]. The feasibility of this has been demonstrated using large area hemispherical phased array transducers, which allows reduction of the energy density at the skull surface.

The first proposal to use focused ultrasound in ophthalmology came from Lavine et al. [40] who demonstrated cataract formation when the lens of the eye was targeted. Further experimental studies demonstrated that HIFU can decrease intra-ocular pressure [41], and produce lesions in the vitreous, lens, retina and choroid [42–46]. High intensity focused ultrasound has been used successfully in the treatment of glaucoma. This was first established in experimental models [44, 47] using intensities up to $2000\,W\,cm^{-2}$ at 4.6 MHz. Histology showed focal thinning of the sclera, and focal disruption of the ciliary body with the conjunctiva remaining intact. The first human treatments, undertaken in 1982, gave encouraging results. Of the 880 patients treated, 79.3% had a sustained lowered intra-ocular pressure after 1 year [48]. High intensity focused ultrasound has also been used with success in experiments to seal traumatic capsular tears [43], and in laboratory treatment of intra-ocular tumours [49, 50], retinal detachment [51] and vitreous haemorrhage [42]. Although HIFU has shown considerable promise in these ophthalmological applications, laser surgery has enjoyed wider success and application, presumably because of its apparently simpler technology and application.

Overview of clinical usage

The ability of modern technology to provide real-time images with excellent spatial resolution and contrast has opened a wide window of opportunity for techniques, such as HIFU, which can only be used to full advantage if they can accurately target the tissue volume to be destroyed. Thus, both ultrasound and MRI have been used to guide and monitor HIFU treatments.

The ability of HIFU to target subcutaneous tissue volumes has made it an attractive potential therapy for deep-seated soft tissue tumours. Malignant cancers of the liver, kidney, breast and pancreas have been successfully targeted. While ultrasound does not significantly penetrate bone, many osteosarcomas break through the bone cortex, and are thus good candidates for HIFU treatment. Where bowel gas lies in the propagation path, care must be exercised to avoid it, or steps taken to displace it. In some treatment orientations this may be successfully achieved using the applied pressure from a water balloon placed against the abdomen. HIFU has proved to be an attractive technique for the treatment of uterine fibroids [52–54]. These may be clearly visualised on MR or Ultrasound (US) imaging. While the treatment of benign masses does not necessitate the achievement of confluent tissue ablation, the best prognosis appears to be for those for which the majority of the tumour is targeted [55].

Trans-rectal HIFU treatment of prostate tumours has been widely investigated. Both benign prostate hyperplasia (BPH) and prostate cancer have been targeted. Initial results from clinical trials for treatment of BPH [56, 61] were encouraging, with increase in flow rate and decreases in post-void residual volume. However, the long-term results of Madersbacher et al. [62] were disappointing, with 43.8% of patients requiring a salvage trans-urethral resection of the prostate (TURP) within 4 years, thus HIFU has not proved significantly better than the ''gold standard'' treatment (TURP). Treatment of cancer in the prostate presents different problems from those associated with the treatment of BPH. [58, 63–67]. Prostate cancer is a multi-focal disease, the foci of which are difficult to detect with diagnostic ultrasound. It is important for its control that all foci are destroyed. The most successful HIFU treatments have been those that have ablated the whole gland [68–72]. Madersbacher et al. [58] were the first to report successful treatment of whole glands. With experience, control rates for the treated tumour have risen from 50% at 8 months in the early days to 90% more recently [64, 72]. Mid-term follow-up (2–5 years) has shown that the prostate specific antigen, (PSA) levels remain low and that the negative biopsy rate remains around 90% [73–78].

There is little in the way of conventional therapy to offer patients whose prostate cancer recurs after radiation therapy. High intensity focused ultrasound may be able to fulfil this role as it offers selective tissue destruction without side effect. Early trials for this application have shown encouraging results [79, 80].

The trans-rectal probe has been used as an extra-corporeal source to treat testicular cancer in the solitary testis with up to 5 years of follow up [81].

Physical principles

Ultrasound propagation through tissue

An ultrasound wave emanating from a transducer outside the body must travel through multiple tissue layers, (including skin, subcutaneous fat, muscle), prior to reaching the desired treatment site within the target organ. At each tissue interface, part of the energy carried by the sound wave will be reflected, whilst the remaining energy is transmitted. The transmission coefficient depends primarily on the difference in acoustic impedance, Z, defined as the product of density and speed of sound, between

the two tissue layers, as well as on the thickness of each layer [82]. At interfaces where there is little difference in acoustic properties, the transmission coefficient is close to unity. With the exception of fat, air and bone, most tissues in the human body have acoustic properties similar to those of water. Aqueous media are therefore optimal for transmitting ultrasound energy from the transducer into the body, and reflections at tissue interfaces are generally weak.

Furthermore, when ultrasound propagates through a particular tissue layer, the pressure fluctuations induced lead to shearing motion of tissue at a microscopic level, which results in frictional heating. Part of the mechanical energy carried by the incident wave is thus converted into heat by this viscous absorption, which constitutes the primary mechanism for ultrasound-induced hyperthermia. In an inhomogenous medium, small regions with different acoustic properties from their surroundings will scatter the incident wave in all directions, causing a loss of acoustic intensity in the direction of sound propagation. The loss in incident acoustic energy in a medium is characterised by its attenuation coefficient, μ, given by the sum of the absorption coefficient μ_a and the scattering coefficient μ_s. The ultrasound intensity, I, following propagation through a distance x in a medium of attenuation coefficient μ is given by

$$I = I_0 e^{-\mu x} \quad (1)$$

where I_0 is the incident ultrasound intensity at the origin ($x = 0$).

For most tissues, the attenuation coefficient is related to the ultrasound frequency via a power law of the form

$$\alpha = af^b, \quad (2)$$

where a and b are tissue-specific constants [82]. It is precisely this dependency of attenuation on frequency that renders ultrasound particularly well-suited to non-invasive therapy, but which causes some significant challenges in optimising HIFU-induced hyperthermia. Unlike other hyperthermia modalities, such as radiofrequency RF or microwaves, the attenuation of sound through water-like media at ultrasound frequencies is sufficiently low that adequate amounts of energy can be delivered to the depths through tissue required during clinical treatments. Increasing the ultrasound excitation frequency results in a power-law increase of both the absorption and attenuation coefficient. The former implies that higher heat deposition is achieved, while both result in a decreased penetration depth. Therefore, the optimal choice of therapeutic ultrasound frequency is application-specific, and represents a compromise between treatment depth and the desired rate of heating. Frequencies near 1 MHz have been found to be most useful for heat deposition, with frequencies as low as 0.5 MHz being used for deep treatments and as high as 8 MHz for shallower treatments [83, 84], as shown in Table I.

Tissue-specific values for the constants a and b in Equation 2 have been reported by Duck [85] and Goss [86, 87]. Tissues such as fat and breast are found to have particularly high attenuation coefficients, whilst those of brain and of most abdominal organs are considerably lower. Furthermore, with the exception of fat, the attenuation coefficient for most tissues increases both with increasing temperature [88] and following HIFU ablation [89]. Although this temperature dependence may be exploitable for the purpose of monitoring HIFU therapy, it poses significant challenges in planning HIFU treatments.

For reasons of convenience, ultrasound therapy studies are often conducted in tissue-mimicking

Table I. Characteristics of transducers in use for clinical applications of HIFU.

Device type	Application	Guidance	Frequency	Transducer aperture	Focal length	Acoustic power	Intensity	Reference
E-C	Liver cancer	US	0.8/1.6 MHz	12 cm	135 mm		5×10^3–20×10^3 W cm^{-2}	[154]
E-C	Kidney cancer	US	0.8/1.6 MHz	12 cm	13.5 mm	<300 W		[155]
E-C	Breast cancer	US	1.6 MHz	12 cm	90 mm		5×10^3–15×10^3 W cm^{-2}	[156]
E-C	Uterine fibroid	MR	0.96–1.14 MHz	12 cm	Variable	100–140 W		[53]
E-C	Osteosarcoma	US	0.8 MHz	12 cm	135 mm	80–160 W	2×10^3–8×10^3 W cm^{-2}	[157]
E-C	Pancreatic cancer	US	0.8 MHz	12 cm	135 mm	<300 W	5×10^3–20×10^3 W cm^{-2}	[158]
T-R	Prostate BPH	US	4 MHz	30 × 22 mm	30–40 mm		1.3×10^3–2.0×10^3 W cm^{-2}	[159]
T-R	Prostate cancer	US	4 MHz		30–50 mm		1.3×10^3–2.2×10^3 W cm^{-2}	[160]
T-R	Prostate cancer	US	3 MHz	61 mm × 39 mm	45 mm	26–35 W		[79]
I-C	Rhinitis	None	5–8 MHz	5 mm	2–3 mm	10–20 W		
I-C	Biliary duct cancer	US	10 MHz	3 mm × 10 mm	n/a	–	14 W cm^{-2}	[147]
H/H	Gynaecology	None	5–8 MHz	12 mm	5 mm	10–30 W		[161]

E-C: Extra-corporeal; T-R: Trans-rectal; I-C: Intracavitary; H/H handheld.

materials, or phantoms, which are generally designed to have similar density, speed of sound and attenuation properties to human tissue [90–93]. However, the absorption coefficient, coefficient of nonlinearity and minimum single-cycle pressure amplitude required to generate cavitation (also known as the cavitation threshold) in such phantoms are generally considerably lower than those of tissue. Even though tissue-mimicking materials provide a much-needed reproducible medium in which to conduct mechanistic studies and characterise HIFU fields under known propagation conditions, it must be noted that any observed temperature changes are unlikely to be directly transferable to perfused tissue.

Linear and nonlinear heating effects

In most clinical applications, HIFU transducers are excited sinusoidally at a single frequency in the range 0.5–8 MHz. If the resulting sound wave propagates linearly through tissue, then heating rates depend on the incident ultrasound intensity and the absorption coefficient locally. The effective heating rate can thus be estimated using a standard heat conduction equation possessing both source and sink terms to account for ultrasound heating and heat loss due to vascular perfusion [87, 94–96].

However, the frequency dependence of the absorption coefficient implies that any nonlinear mechanisms that give rise to higher frequency components in the sound field will also yield enhanced heating. Two such mechanisms can be readily identified: Nonlinear wave propagation [97] and cavitation [98].

When a large-amplitude single-frequency sound wave propagates through a nonlinear medium, the waveform becomes gradually shocked, resulting in the leakage of energy from the fundamental frequency into its higher harmonics, as illustrated in Figure 2. The extent to which such leakage occurs depends on the amplitude of the incident wave, on the nonlinearity of the medium, generally described by the parameter B/A, and on the distance travelled by the wave into the medium. The parameter B/A is proportional to the ratio of coefficients of the quadratic and linear terms in the Taylor series expansion of the variations of the pressure B/A for most soft tissues is close to that of distilled water, but for fat is almost twice that of any soft tissue [97]. In the context of HIFU, nonlinear effects become increasingly significant as the depth of treatment is increased, or if a region of high intensity happens to be coincident with a layer of fatty tissue, as illustrated in a medium in terms of the variations of the density under isentropic conditions [97]. The speed of sound, c, of a large-amplitude plane wave in a given medium is related to the speed c_0 of a small-amplitude wave in the same medium by $c = c_0 + 0.5(B/A)u$, where u is the particle velocity. Physically, the parameter B/A therefore determines the relative importance of the leading-order finite-amplitude correction to the small-signal sound speed c_0 and thus also determines the shock formation distance for a plane wave that is sinusoidal at the source [97].

The parameter B/A for most soft tissues is close to that of distilled water, but for fat is almost twice that of any soft tissue [97]. In the context of HIFU, nonlinear effects become increasingly significant as the depth of treatment is increased, or if a region of high intensity happens to be coincident with a layer of fatty tissue (Figure 2). Generally, at the intensities used in HIFU, nonlinear propagation is a significant contributor to the heating observed.

At large amplitudes, the peak rarefaction pressure of an ultrasound wave may be sufficiently large for small cavities, which contain vapour as well as some of the gas originally dissolved in the surrounding medium, to form. Cavity formation could also arise from thermal effects alone, when the temperature in the tissue approaches boiling temperatures, resulting in the formation of (generally large) vapour bubbles. The behaviour of all such cavities under the influence of a sound field is known as acoustic cavitation, which is generally classified into stable and inertial [98]. The type of cavitational activity observed depends, to first order, on the bubble size compared to the linear resonance size at the frequency of insonation [98] and on the relative contribution of vapour and gas pressures to the total pressure inside the bubble [99] Stable cavitation describes the sustained oscillations of cavities whose size is normally close to, or greater than, the resonant size for the insonation frequency, which can result in period-doubling oscillations of the cavity wall. Inertial cavitation describes the explosive growth of a cavity of initial size about a third of resonant size, and its subsequent violent collapse under the effect of the inertia of the surrounding fluid. Inertial collapses typically occur over a single or a small number of acoustic cycles and result in broadband noise emissions.

The significance of cavitation for enhanced heating has been widely acknowledged [99–106] and can broadly be attributed to two main mechanisms. If the pressure amplitude is sufficiently large for cavitational activity, whether stable or inertial, to exist in a volume of tissue, then strong scattering of the incident wave by these multiple bubbles results in acoustic energy being ''trapped'' within the cavitating region. This results in enhanced heating in that region due to viscous absorption of the trapped excess energy. In the case of inertial cavitation alone, the violent bubble collapse results in a redistribution

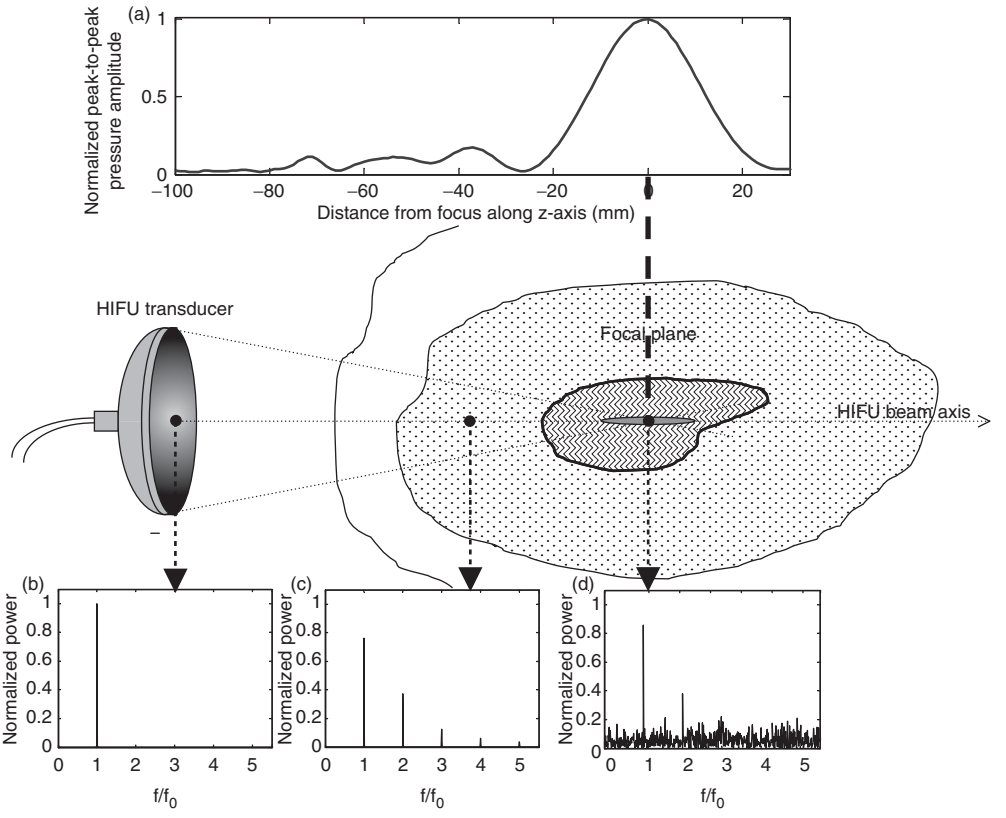

Figure 2. Superposition onto the HIFU treatment geometry of a typical axial HIFU pressure profile (a) and of a diagrammatic representation of the frequency-content, f, of the HIFU wave (b–d) as it propagates through tissue. (a) Representative axial pressure distribution (characterised using a hydrophone in water) for a typical HIFU transducer. The large peak defines the focal region of the HIFU transducer, within which thermal damage is expected to occur. Prefocal peaks can also be seen to exist which, should they overlap with a tissue region that is either highly nonlinear or has a high absorption coefficient, are likely to cause significant prefocal heating. The HIFU transducer is generally excited sinusoidally with a single frequency, f_0, resulting in a monochromatic wave (b). As this wave travels through a nonlinear medium, superharmonic leakage occurs (c) and energy at these higher harmonics is readily absorbed and converted into heat. Finally, if inertial cavitation occurs (generally, but not necessarily, in the focal region), the collapsing microbubbles convert part of the incident energy into broadband noise emissions (d), which are very rapidly and very locally absorbed and converted into heat.

of the energy received by the bubble at the fundamental HIFU frequency into broadband noise emissions, as shown in Figure 2. The frequency dependence of the absorption coefficient implies that high-frequency emissions are more readily absorbed and attenuated, leading to enhanced heat deposition in the immediate vicinity of the inertially cavitating bubble. In a HIFU field, a region over which cavitation occurs can thus be perceived as having an increased effective absorption and attenuation coefficients. Furthermore, the presence of bubbles will result in a change in the acoustic impedance of the tissue volume, yielding larger reflection coefficients at the boundaries of the cavitating region. In any given medium, the relative increase in any of those coefficients will depend primarily on the bubble number density, the range of bubble sizes and the type of cavitation activity being excited.

Much effort has been expanded in assessing the relative importance of enhanced heating due to nonlinear propagation and cavitation, either by attempting to suppress cavitation activity by use of overpressure, and can broadly be attributed to two main mechanisms. If the pressure amplitude is sufficiently large for cavitational activity, whether stable or inertial, to exist in a volume of tissue, then strong scattering of the incident wave by these multiple bubbles results in acoustic energy being ''trapped'' within the cavitating region. This results in enhanced heating in that region due to viscous absorption of the trapped excess energy, arising primarily in the viscous boundary layer between the bubble and the surrounding medium. In the case of inertial cavitation alone, the violent bubble collapse results in a redistribution of the energy received by the bubble at the fundamental HIFU frequency into

broadband noise emissions. The frequency dependence of the absorption coefficient means that high-frequency emissions are more readily absorbed and attenuated, leading to enhanced heat deposition in the immediate vicinity of the inertially cavitating bubble. In a HIFU field, a region over which cavitation occurs can thus be perceived as having increased effective absorption and attenuation coefficients. Furthermore, the presence of bubbles will result in a change in the acoustic impedance of the tissue volume, yielding larger reflection coefficients at the boundaries of the cavitating region. In any given medium, the relative increase in any of those coefficients will depend primarily on the bubble number density, the range of bubble sizes and the type of cavitation activity being excited [99].

Much effort has been expended in assessing the relative importance of enhanced heating due to nonlinear propagation and cavitation, either by attempting to suppress cavitation activity by use of overpressure or by investigating the heating generated by various cavitational regimes both theoretically and experimentally, and on the effect of the viscoelastic properties of tissue on bubble dynamics and on the effect of the viscoelastic properties of tissue on bubble dynamics. Furthermore, the effect of changes in tissue temperature on cavitation thresholds and bubble activity remains poorly understood. However, it is known that at temperatures approaching the boiling point of water, inertial bubble collapses will be prevented by the increasing vapour pressure.

In tissue, at the intensities currently being employed clinically for HIFU treatment, it is likely that both inertial cavitation and nonlinear propagation play a significant role. At a given pressure amplitude, the relative contribution of these two mechanisms will depend on the cavitation threshold, the tissue temperature, the distance over which ultrasound has propagated and the B/A of tissues lying in the ultrasound propagation path.

Exposure parameters and dosimetry

In medical applications of ionising radiation, a distinction is clearly made between ''exposure'' and ''dose''. Exposure in this context is the amount of ionisation produced in air by X- or γ-rays. The unit of exposure is the Roentgen, R, (the quantity of ionising radiation that will produce one electrostatic unit of electricity in one cubic centimetre of dry air at 0°C and standard atmospheric pressure.). This is a measure of the amount of radiation that reaches the body, but does not describe the fraction of that incident energy that is absorbed within tissue. Radiation physicists defines a second parameter for this, the ''absorbed dose'' (commonly referred to as ''dose''). This characterises the amount of energy deposited per kilogram. The units for dose are the gray (Gy) and the rad, where 1 rad = 100 Gy. The dose as defined in this fashion does not distinguish between different types of radiation. A weighting factor (relative biological effect, RBE) is used in an attempt to compare the biological effects of different forms of ionising radiation. This leads to a ''dose equivalent'' parameter, whose units are the rem or sievert, Sv, (1 rem = 100 Sv). These parameters are related by the equation:

$$\text{Dose equivalent (Sv)} = \text{dose (Gy)} \times \text{RBE}. \qquad (3)$$

X-rays, γ-rays and β particles have an RBE of 1.0, whereas α particles have an RBE of 20.

The discipline of medical ultrasound has never drawn these distinctions. The terms ''exposure'' and ''dose'' are used interchangeably in the literature, although a cogent case for adopting the distinction can be made. Differing biological consequences may result from different modes of ultrasonic energy delivery. For example, two exposures which use the same total acoustic energy over an identical time span, where one is delivered in continuous mode, and the other in short pulses at low repetition rate, may result in very different effects in tissue. The first is more likely to induce thermal effects, while the second may stimulate cavitation activity and its associated characteristic cell damage. In making the transition from exposure to dose in an ultrasound field, it is necessary to know the acoustic parameters of the propagation path. The acoustic parameters of most interest in this context are attenuation and absorption coefficients, the speed of sound and the nonlinearity parameter B/A. These parameters are often not well-characterised, and large gaps in knowledge exist for normal and malignant human tissues, and for the temperature dependence of such parameters.

Conventionally, ultrasound exposures are characterised in terms of the acoustic field determined under free field conditions in water. ''Free field'' for these purposes describes circumstances in which the ultrasound beam propagates freely, with no influence from boundaries or other obstacles. The parameters necessary for description of HIFU exposures are frequency, exposure time, transducer characteristics, total power, acoustic pressure and/or intensity (energy flux in Watts cm^{-2}) and energy delivery mode (single shots, scanned exposures, etc.). The total output power is usually determined using a radiation force balance method [107, 108]. The force measured depends on focusing and other aspects of the field geometry, the target shape and properties. Other important factors affecting the measurement

are the distance of the target from the source, absorption of energy in the water path between the transducer and the target, and acoustic streaming currents. Other methods of power measurement are under investigation, with the most promising being the use of the pyro-electric properties of PVDF membranes [109]. Shaw has also described the use of the change in buoyancy of a castor oil target heated by an incident high power ultrasound beam for the determination of acoustic power. This method is thought to be particularly useful when very strongly focused transducers (f-number less than 1.5) and phased arrays are being characterised.

Acoustic pressure is measured using a hydrophone. Both needle and membrane hydrophones have been used [110–116]. Membrane hydrophones have the advantage of only minimally disturbing the field, but may be damaged by pressures high enough to induce cavitation at their surface. Beam profiles are usually measured at much lower output levels than are used for clinical HIFU treatments for this reason, and it is assumed that a linear extrapolation to higher levels is valid. This method introduces errors since it ignores the effects of nonlinear propagation which occur at high pressures. Once the position of the focal peak has been established using a hydrophone, the peak acoustic pressure amplitude can be measured. From this the spatial peak (focal peak) intensity can be calculated. The beam width can be determined from the pressure distribution. It is also possible to obtain spatial information about a HIFU beam by scanning a thermocouple embedded in an absorbing medium through the field, or by use of Schlieren imaging.

A number of different parameters have been used to describe a HIFU field. Generally exposures are described in terms of free field water measurements. In some cases, an attempt is made to calculate an *in situ* intensity using an estimation of the total attenuation in the beam path. Spatial peak (focal peak) intensities and spatially averaged intensities are also sometimes quoted. Hill et al. [117] have attempted to define a parameter that may usefully predict the intended outcome of a HIFU exposure – namely ablation. In an ultrasound beam that is propagating nonlinearly through a medium, energy is transferred from the fundamental frequency to harmonics, with consequent changes in both beam shape and effective absorption coefficient. The boundary of an ablative region occurs where the combination of temperature and time has exceeded a required threshold. Hill et al. define a parameter, I_{SAL}, which is the acoustic intensity spatially averaged over the area enclosed by the half pressure maximum contour as determined under linear conditions. This parameter has the merit that the acoustic power can be measured at clinically relevant levels, while the beam profile is measured under linear (low output) levels for which hydrophones can be safely used. It can be shown that I_{SAL} is 0.557 times the intensity at the spatial pressure maximum of the linear beam profile. The contour at half the pressure maximum is taken as being representative of the lesion cross-section. While nonlinear propagation is known to narrow the beam profile, thermal diffusion will broaden it, thus reducing the impact of the inaccuracies introduced by the linear measurement conditions. Hill et al. demonstrated that there was a correlation between lesion diameter and I_{SAL}. However, it is unlikely to be satisfactory for beams carrying significant amounts of energy in the side lobes, such as phased arrays, especially when they are firing off axis.

Clinically, the most useful dose parameter is likely to be one that gives a measure of the volume rate of tissue destruction (cc/unit time). It is therefore necessary to be able to relate the ablated tissue volume to measurable field and other parameters. Two dose parameters related solely to thermal effects have been proposed. A thermal dose parameter has been proposed by Sapareto and Dewey [118]. This has been extensively used to describe hyperthermia treatments for cancer therapy. The temperature-time history for a particular tissue volume is integrated and reduced to an equivalent exposure time at 43°C. The equivalent time t_{43} is given by the equation

$$t_{43} = R^{(T-43)}\Delta t, \tag{4}$$

where R is 0.5 above 43°C and 0.25 below 42°C, and T is the average temperature over a time Δt. This has been shown to be valid up to about 50°C, but is difficult to validate experimentally at the short times required above this temperature since very fast heating rates are required. An alternative parameter related to the heating potential of the HIFU beam is the product of intensity and time (a measure of the total energy).

It is now well-accepted that cavitation can enhance the heating in a HIFU field [100–106]. Cavitation may be detected from the acoustic emissions generated (subharmonic, harmonic, superharmonics and broadband signals) and may be visualised on diagnostic ultrasound scans. However, there is, as yet, no validated method of quantifying cavitation activity, nor accepted method for defining ''cavitation dose''.

Table I lists the characteristics of transducers currently in clinical use. The aim for most systems is to deliver an *in situ* intensity of greater than $10^3\,W\,cm^{-2}$ at the focus. For extra-corporeal sources with long focal length, this is achieved using a wide aperture source driven at high power. Wide aperture sources have the advantage of distributing the

incident energy over a large skin area, thus reducing the possibility of skin burn. Trans-rectal and intracavitary sources operate at lower powers and higher frequencies as they can be placed close to the target volume.

Devices

The treatment process

Effective HIFU treatments depend on the successful conduct of a number of different stages of the procedure. For cancer, the initial diagnosis is usually made from CT or MR scans. An assessment of the tumour's visibility to diagnostic ultrasound is then required. This involves ascertaining that there is a suitable acoustic window through which the treatment can be delivered, that the target boundaries can be clearly identified, and that no sensitive normal tissue structures lie in the beam path. The target volume must be accurately identified and spatially localised. The second stage in the treatment is to determine the correct ultrasound exposure to achieve ablation. This is done in a number of ways. Where ultrasound imaging is used for guidance, the most common method is to use a combination of focal peak intensity and exposure time that results in a hyperechoic region at the target, whereas when MR is the guidance method, this combination is varied until the required temperature (and hence thermal dose), as seen using MR thermometry, is reached.

During the treatment delivery phase, some indicator of tissue change is desirable. This enables assessment of treatment progress, and may also provide feedback to allow adjustment of exposure parameters in real time. A number of different indicators have been used. For MR guided HIFU, the temperature rise may be determined using spin-lattice relaxation time (T_1), proton resonance frequency (PRF) or proton diffusion (D) related sequences [119]. For US guided treatments, the most commonly used indicator of tissue ablation is the appearance of a hyperechoic region on the image, but other techniques such as elastography and ultrasound thermometry are under active investigation [119].

The final component of the HIFU procedure is post-treatment assessment of the extent of tissue ablation. Contrast enhanced MR and ultrasound imaging allow visualisation of vasculature. Successful HIFU ablation leads to occlusion of blood vessels in the target volume, and thus reduced contrast uptake following treatment [120].

Treatment delivery

The guiding principle of HIFU is that an ultrasonic beam should be able to destroy a sharply defined region of tissue rapidly, with minimal effects to surrounding tissues. Focusing of the ultrasound beam may be achieved in a number of ways. The simplest method is to use a single element spherical shell of piezo-electric material capable of delivering high power. Whereas quartz was the transducer material of choice in the early days of HIFU, recent developments have seen the use of piezo-ceramics such as PZT (lead zirconate titanate) and piezo-composite materials. The single element focused bowl transducer gives no flexibility as to focal length. Different focal lengths may be achieved by combining a plane single element transducer with lenses of different specifications. Lenses are usually made from materials having a speed of sound greater than that of water, and thus are of concave shape when a convergent beam is sought. Good impedance matching is required in order to minimise energy loss at the transducer–lens interface. Maximum transmission is obtained when the transducer and lens are separated by a quarter wavelength of impedance matching material. Fry [121] achieved energy localisation by using four plane transducers each fronted by a plano-concave lens. The beams were arranged in such a way that their foci overlapped, and the intensity was maximised by optimal phasing of the individual beams. This method requires the availability of four separate acoustic windows.

Emerging phased array technology for high powered ultrasound applications has led to the design of transducers that allow electronic beam steering to facilitate more rapid treatment of clinically relevant volumes [122–134]. Transducers for clinical use fall into three main classes: Extracorporeal, trans-rectal and endoscopic. Extra-corporeal transducers are used for targeting organs that are readily accessible through an acoustic window on the skin, whereas trans-rectal devices are used for the treatment of the prostate and endoscopic probes are being developed for the treatment of biliary duct and oesophageal tumours.

The acoustic energy may be delivered in a number of ways. A single exposure (typically 2–10 s of duration) may be made with the transducer held stationary. This results in a well-demarcated ''lesion'' of dimensions determined by the focal region of the transducer. Where larger volumes are to be targeted, the transducer may be moved in discrete steps, and fired at each position, where the distance between ''shots'' will determine whether lesions are overlapping or separate, depending on the necessity to achieve confluent regions of cell killing (Figure 3). An alternative exposure strategy is to move the active therapy transducer in pre-determined trajectories (e.g. linear tracks or spirals) to conform with the required treatment volume. If the correct combination of transducer velocity and ultrasound energy is

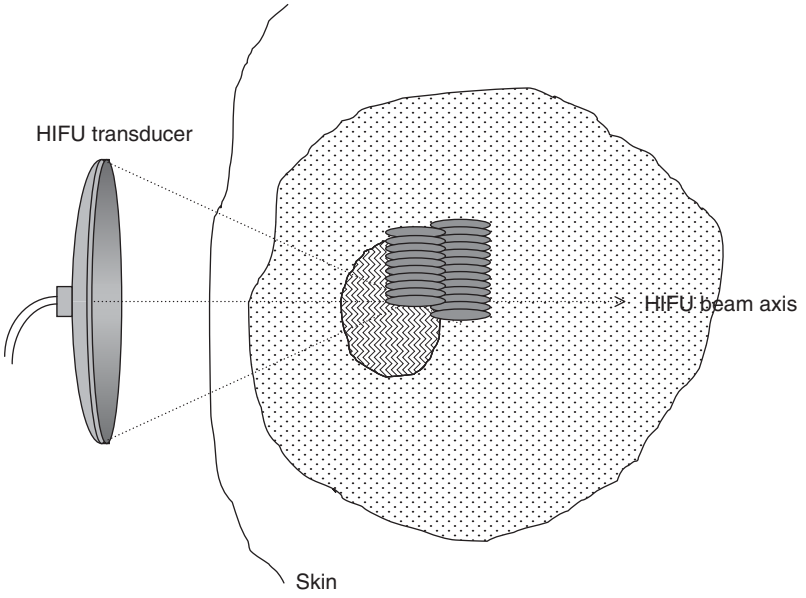

Figure 3. Diagrammatic illustration of HIFU treatment delivery for the ablation of large tissue volumes. Multiple lesions are created side-by-side to span the required treatment volume, starting on the side distal to the transducer. The lesions can be overlapping or separate, depending on the necessity to achieve confluent regions of cell killing.

used, these result in confluent volumes of cell damage.

Extracorporeal devices

Tissue targets lying within the breast, abdomen, brain or limbs are usually treated using an extracorporeal HIFU source. Trans-cutaneous treatments of this nature require that there is a suitable acoustic window on the skin that provides a propagation path for the focused beam that is uninterrupted by intervening gas. In addition, it must be possible to couple the ultrasound energy to the skin surface using coupling gel, a water balloon or other suitable liquid path.

Extracorporeal HIFU treatments are guided using either US or MRI. These methods are reviewed by Rivens et al. [119].

For operation in the high magnetic fields used for MRI, HIFU transducers must be specially designed for compatability with such fields. The PZT material commonly used for HIFU transducers contains Nickel, which is necessary for the high levels of electrical excitation and mechanical stress induced. However, Nickel causes magnetic field distortion. In addition, eddy currents may be set up in the conductive silver coating of transducers. These eddy currents may cause local magnetic field inhomogeneities, and significant image artefacts. Eddy currents can be reduced by segmenting the transducer face into a number of areas [135]. These problems are considerably reduced by the new piezo-composite materials available. The Exablate© (Insightec Ltd, Israel) system uses a 208 element phased array transducer with the elements arranged to form the surface of a spherical bowl. Suitable phasing of the drive signal to these elements allows a complex pressure distribution to be achieved in the focal region, with the intention of allowing thermal conduction between spatially separated pressure peaks to produce a larger zone of tissue destruction than would be possible if all transducer elements were driven in phase with each other. Using MR thermometry, this system enables calculation of thermal dose, and superimposes a representation of the regions in which the thermal dose has achieved cytotoxic levels on the anatomical MR image. Using this type of display, the entire target region can be ''painted'' out during treatment.

Where US is used to guide and monitor HIFU treatments, the diagnostic transducer is incorporated into the treatment head. This allows real time imaging of the ablation process. The thermally ablated region is not visible on standard B-mode images unless gas bubbles have been induced. HIFU exposures levels are therefore often adjusted until a hyperechoic region is seen on the US image, indicating that bubbles are present in this region. It is not, as yet, clear whether these are generated by acoustic cavitation or by thermal exsolution of tissue gas. Elastographic techniques will allow treatments to be monitored in real time since the stiffness of tissue is altered by the ablation process [136–138]. However, this technique has not yet achieved widespread clinical use. The speed of sound provides is temperature dependent, and thus imaging

techniques that make use of this phenomenon may be employed to locate and place the focus using a low powered ''siting'' shot. The apparent change in position of echoes, when images of heated and unheated tissues are compared, is due to these changes in sound speed. The speed of sound vs. temperature curve for soft tissues exhibits a peak around 55°C, and thus this is not a useful technique for detecting threshold ablation temperatures, although a number of researchers are looking for ways around this [139].

Trans-rectal devices

The trans-rectal devices that have been developed for the treatment of benign and malignant prostate disease have probes that can be inserted *per rectum* and which incorporate both imaging and therapy transducers in one unit [60, 68, 140–145]. The two commercially available devices, the Ablatherm© (Edap Technomed, France) and the Sonablate™ (Focus Surgery, USA), are very similar in concept. Both systems incorporate therapy and imaging transducers into a treatment head mounted at the end of a trans-rectal probe. The therapy transducer takes the form of a truncated spherical bowl. The clinical aim of both devices is usually to ablate the entire prostate, although nerve sparing treatments are sometimes required. Prostate ablation is achieved by placing touching lesions side by side. In the Ablatherm© device, lesion length is varied by adjustment of the ultrasound power to pre-set levels, whereas for the Sonablate™ the thicker prostates are ablated using two layers of lesions, the deeper layer being created using a longer focal length than the more superficial layer. The different focal lengths are achieved by rotating the transducer, the two sides having different geometries. Sonablate™ users are able to vary the acoustic output power of the probe.

Interstitial devices

There has been some interest in the development of high intensity ultrasound probes for interstitial use. In the main, these use plane transducers rather than focusing elements, and volume destruction is obtained by rotation of the probe. Prat et al. [146, 147] have described a probe designed for the intra-ductal treatment of biliary tumours. A 3 mm × 10 mm 10 MHz plane transducer is mounted on a stainless steel shaft that is passed through a jumbo fiberduodenoscope. The probe can be positioned under fluoroscopic guidance. An ultrasound intensity at the transducer face of 14 W cm^{-2} is used for 10–20 s bursts. Circumferential ablation is achieved by rotation of the flexible probe. The transducer is rotated by 18° after each ''shot''. Once 360° of damage has been achieved the probe is repositioned under fluoroscopic guidance to create adjacent rings, each 8 mm in height. This has been used clinically with some encouraging results [148, 149].

A similar device has been created for the treatment of oesophageal tumours [150]. A 15 mm × 8 mm 10 MHz piezoceramic plane transducer is mounted on an 80 cm long, 10 mm outside diameter flexible shaft. Intensities of 12–16 W cm^{-2} for exposure times of 5–20 s gave ablation to a maximum depth of 13 mm in *ex vivo* liver. In the oesophagus *ex vivo* a 10 s exposure at 12 W cm^{-2} resulted in damage to a depth of 4–5 mm. A similar MR compatible device has been developed.

Makin et al. [151] have also developed a probe for percutaneous and laparoscopic treatment of the liver. The probe consists of a (32 3.1MHz) element imaging and therapy array with 2.3 mm elevation, 1.53 mm pitch and 49 mm aperture. Intensities of 60–80 W cm^{-2} at the surface of the transducer leads to ablation rates of ~2 ml/min to a depth of 30–40 mm. Rotational treatments can be undertaken.

The ability of high intensity ultrasound beams to occlude the blood supply and coagulate tissue has been exploited in the design of a device to allow bloodless partial nephrectomy [153]. A 3.8 MHz 1.2 cm^2 plane transducer mounted on a handheld applicator is used at an intensity at the transducer face of 26 W cm^{-2}. Full thickness tissue coagulation in the pig kidney was achieved.

Discussion and conclusions

The drive in modern medicine is towards the development of treatments and techniques that minimise intervention to the patient and length of hospital stay. Thermal ablation therapies provide a minimally invasive approach to cancer therapy that is gaining rapid clinical acceptance. Of the available ablative techniques, HIFU is the least invasive, and as such is, in many ways, the most attractive. HIFU is, however, still in its infancy, and there remain outstanding technical and treatment delivery questions to be addressed.

While the prime mechanism for cellular destruction by HIFU, namely heating, is largely understood, the role of cavitation is still to be fully elucidated. Even though bubble activity at the focus may aid treatment monitoring and enhance ultrasonic heating, cavitation occurring pre-focally may lead to unwanted cell damage in overlying tissue volumes. Methods of cavitation control are under active investigation [99, 162].

The move from single element ultrasound sources to multi-element phased arrays allows more rapid

scanning of the focus through tissue, and greater flexibility in focal geometry. It is becoming apparent that there are some clinical applications for which the design of specific HIFU probes is beneficial (as already seen for the prostate, bile duct and oesophagus). This is likely to be the case for targets lying close to sensitive tissues that must be spared, and for those that are best imaged using specialist techniques.

The increasing complexity of HIFU sources and treatment delivery regimes has implications for treatment planning. A comprehensive knowledge of tissue acoustic and thermal properties is necessary, both at normothermic and elevated temperatures. It is becoming apparent that HIFU is establishing its role in clinical usage, especially in cancer therapy. The long-term results still to be obtained from treatments that have already been carried out will clarify the applications for which it will give the greatest benefit. However, with improving imaging and energy delivery techniques, it is probable that the versatility of HIFU will increase, and its range of applicability will expand.

References

1. Sapareto DG, Dewey WC. Thermal dose determination in cancer therapy. Br J Radiation Oncology Biol Phys Med 1984;10:787–800.
2. Dewhirst MW, Viglianti BL, Lora-Michiels M, Hanson M, Hoopes PJ. Basic principles of thermal dosimetry and thermal thresholds for tissue damage from hyperthermia. Int J Hyperther 2003;19:267–294.
3. Fosse E. Thermal ablation of benign and malignant tumours. Minim Invasive Ther Allied Technol 2006;15:2–3.
4. Lee JM, Han JK, Chang JM, Chung SY, Son KR, Kim SH, Lee JY, Choi BI. Radiofrequency renal ablation: *In vivo* comparison of internally cooled, multitined expandable and internally cooled perfusion electrodes. J Vasc Interv Radiol 2006;17:549–556.
5. Papagelopoulos PJ, Mavrogenis AF, Galanis EC, Kelekis NL, Wenger DE, Sim FH, Soucacos PN. Minimally invasive techniques in orthopedic oncology: Radiofrequency and laser thermal ablation. Orthopedics 2005;28:563–568.
6. Nikfarjam M, Muralidharan V, Su K, Malcontenti-Wilson C, Christophi C. Patterns of heat shock protein (HSP70) expression and Kupffer cell activity following thermal ablation of liver and colorectal liver metastases. Int J Hyperther 2005;21:319–332.
7. Lee JM, Han JK, Kim SH, Han CJ, An SK, Lee JY, Choi B. Wet radio-frequency ablation using multiple electrodes: Comparative study of bipolar versus monopolar modes in the bovine liver. Eur J Radiol 2005;54:408–417.
8. Onishi H, Matsushita M, Murakami T, Tono T, Okamoto S, Aoki Y, Iannaccone R, Hori M, Kim T, Osuga K, et al. MR appearances of radiofrequency thermal ablation region: Histopathologic correlation with dog liver models and an autopsy case. Acad Radiol 2004;11:1180–1189.
9. Galandi D, Antes G. Radiofrequency thermal ablation versus other interventions for hepatocellular carcinoma. Cochrane Database Syst Rev 2004;2:CD003046.
10. Izzo F. Other thermal ablation techniques: Microwave and interstitial laser ablation of liver tumors. Ann Surg Oncol 2003;10:491–497.
11. Puls R, Stroszczynski C, Gaffke G, Hosten N, Felix R, Speck U. Laser-induced thermotherapy (LITT) of liver metastases: MR-guided percutaneous insertion of an MRI-compatible irrigated microcatheter system using a closed high-field unit. J Magn Reson Imaging 2003;17:663–670.
12. Ng KK, Lam CM, Poon RT, Ai V, Tso WK, Fan ST. Thermal ablative therapy for malignant liver tumors: A critical appraisal. J Gastroenterol Hepatol 2003;18:616–629.
13. Pacella CM, Bizzarri G, Magnolfi F, Cecconi P, Caspani B, Anelli V, et al. Laser thermal ablation in the treatment of small hepatocellular carcinoma: Results in 74 patients. Radiology 2001;221:712–720.
14. Shibata T, Niinobu T, Ogata N. Comparison of the effects of in-vivo thermal ablation of pig liver by microwave and radiofrequency coagulation. J Hepatobiliary Pancreat Surg 2000;7:592–598.
15. Warwick R, Pond JB. Trackless lesions in nervous tissues produced by high intensity focused ultrasound (High frequcncy mechanical waves). J Acoust Soc Am 1968;102: 387–405.
16. Pond JB. The role of heat in the production of ultrasonic focal lesions. J Acoust Soc Am 1970;47:1607–1611.
17. ter Haar GR, Robertson D. Tissue destruction with focused ultrasound in vivo. Eur Urol 1993;23(Suppl. 1):8–11.
18. Hynynen K, Colucci V, Chung A, Jolesz F. Noninvasive arterial-occlusion using mri-guided focused ultrasound. Ultrasound Med Biol 1996;22:1071–1077.
19. Rivens IH, Rowland IJ, Denbow M, Fisk N, ter Haar GR, Leach MO. Vascular occlusion using focused ultrasound surgery for use in fetal medicine. Eur J Ultrasound 1998;00.
20. Susani M, Madersbacher S, Kratzik C, Vingers L, Marberger M. Morphology of tissue destruction induced by focused ultrasound. Eur Urol 1993;23(Suppl. 1):34–38.
21. Vaezy S, Martin R, Yaziji H, Kaczkowski P, Keilman G, Carter S, Caps M, Chi EY, Bailey M, Crum L. Hemostasis of punctured blood vessels using high-intensity focused ultrasound. Ultrasound Med Biol 1998;24:903–910.
22. Vaezy S, Vaezy S, Starr F, Chi E, Cornejo C, Crum L, Martin RW. Intra-operative acoustic hemostasis of liver: Production of a homogenate for effective treatment. Ultrasonics 2005;43:265–269.
23. Vaezy S, Martin R, Kaczkowski P, Keilman G, Goldman B, Yaziji H, Carter S, Caps M, Crum L. Use of high-intensity focused ultrasound to control bleeding. J Vas Surg 1999; 29:533–542.
24. Wu F, Chen WZ, Bai J, Zou JZ, Wang ZL, Zhu H, Wang ZB. Pathological changes in human malignant carcinoma treated with high-intensity focused ultrasound. Ultrasound Med Biol 2001;27:1099–1106.
25. Wu F, Chen WZ, Bai J, Zou JZ, Wang ZL, Zhu H, Wang ZB. Tumor vessel destruction resulting from high-intensity focused ultrasound in patients with solid malignancies. Ultrasound Med Biol 2002;28:535–542.
26. Yang R, Sanghvi NT, Rescorla FJ, Kopecky KK, Grosfeld JL. Liver cancer ablation with extracorporeal high-intensity focused ultrasound. Eur Urol 1993;23(Suppl. 1):17–22.
27. Fallon J.Y. Stehbens WE, Eggleton RC. Effect of ultrasound on arteries. Arch Path 1972;94:380–388.
28. Ishikawa T, Okai T, Sasaki K, Umemura S, Fujiwara R, Kushima M, Ichihara M, Ichizuha K. Functional and histological changes in rat femoral arteries by HIFU exposure. Ultrasound Med Biol 2003;29:1471–1477.
29. Lynn JG, Zwemer RL, Chick AJ, Miller AE. A new method for the generation and use of focused ultrasound in experimental biology. J Gen Physiol 1942;26:179–192.

30. Ballantine HT, Bell E, Manlapaz J. Progress and problems in the neurological applications of focused ultrasound. J Neurosurg 1960;17:858–876.
31. Fry WJ, Fry FJ. Fundamental neurological research and human neurosurgery using intense ultrasound. IRE Trans Biomed Electronics 1960;ME-7:166–181.
32. Lynn JG, Putnam TJ. Histological and cerebral lesions prodcued by focused ultrasound. Am J Pathol 1944;20:637–649.
33. Wall P.D, Fry WJ, Stephens R, Tucker D, Lettvin JY. Changes produced in the central nervous system by ultrasound. Science 1951;114:686–687.
34. Bakay L, Hueter TF, Ballantine HT, Sosa D. Ultrasonically induced changes in the blood brain barrier. A M A Arch Neuro Psychiatr 1956;00:457–467.
35. Fry FJ, Johnson LK. Tumour irradiation with intense ultrasound. Ultrasound Med Biol 1978;4:337–341.
36. Fry WJ, Barnard JW, Fry FJ, Krumins RF, Brennan JF. Ultrasonic lesions in the mammalian central nervous system. Science 1955;122:517–518.
37. Fry FJ, Kossoff G, Eggleton RC, Dunn F. Threshold ultrasound dosages for structural changes in the mammalian brain. J Acoust Soc Am 1970;48:1413–1417.
38. Aubry JF, Tanter M, Pernot M, Thomas JL, Fink M. Experimental demonstration of noninvasive transskull adaptive focusing based on prior computed tomography scans. J Acoust Soc Am 2003;113:84–93.
39. Clement GT, White J, Hynynen K. Investigation of a large-area phased array for focused ultrasound surgery through the skull. Phys Med Biol 2000;45:1071–1083.
40. Lavine O, Langenstrass K, Bowyer C, Fox F, Griffing V, Thaler W. Effects of ultrasonic waves on the refractive media of the eye. Arch Ophthalmol 1952;47:204–209.
41. Rosenberg RS, Purnell E. Effects of ultrasonic radiation on the ciliary body. Am J Ophthalmol 1967;63:403–409.
42. Coleman DJ, Lizzi FL, El-Mofty AAM, Driller J, Franzen LA. Ultrasonically accelerated absorption of vitreous membranes. Am J Ophthalmol 1980;89:490–499.
43. Coleman DJ, Lizzi FL, Torpey JH, Burgess SEP, Driller J, Rosado AL, et al. Treatment of experimental lens capsular tears with intense focused ultrasound. Br J Ophthalmol 1985;69:645–649.
44. Coleman DJ, Lizzi FL, Driller J, Rosado AL, Burgess SEP, Torpey JH, Smith ME, Silverman RH, Yablonshi ME, Chang S, et al. Therapeutic ultrasound in the treatment of Glaucoma – II Clinical Applications. Ophthalmol 1985;92:347–353.
45. Lizzi FL, Coleman DJ, Driller J, Franzen LA, Jackobiec FA. Experimental ultrasonically induced lesions in the retina, choroid, and sclera. Invest Ophthal 1978;17:350–360.
46. Purnell E, Sokollu A, Torchia R, Taner N. Focal chorioretinitis produced by ultrasound. Invest Ophthal 1964;3:657–664.
47. Coleman DJ, Lizzi FL, Driller J, Rosado AL, Chang S, Iwamoto T, et al. Therapeutic ultrasound in the treatment of Glaucoma – I Experimental Model. Ophthalmol 1985;92:339–346.
48. Silverman RH, Vogelsang B, Rondeau MJ, Coleman DJ. Therapeutic ultrasound for the treatment of glaucoma. Am J Ophthalmol 1991;111:327–337.
49. Burgess SEP, Iwamoto T, Coleman DJ, Lizzi FL, Driller J, Rosado AL. Histological changes in porcine eyes treated with high intensity focused ultrasound. Ann Ophthalmol 1987;19: 133–138.
50. Lizzi FL, Coleman DJ, Driller J, Ostromogilsky M, Chang S, Grenall P. Ultrasonic hyperthermia for ophthalmic therapy. IEEE Trans Son Ultrason 1984;SU-31:473–481.
51. Rosecan LR, Iwamoto T, Rosado AL, Lizzi FL, Coleman DJ. Therapeutic ultrasound in the treatment of retinal detachment: Clinical observation and light and electron microscopy. Retina 1985;5:115–122.
52. Chen S. MRI-guided focused ultrasound treatment of uterine fibroids. Issues Emerg Health Technol 2005;70:1–4.
53. Tempany CM, Stewart EA, McDannold N, Quade BJ, Jolesz FA, Hynynen K. MR imaging-guided focused ultrasound surgery of uterine leiomyomas: A feasibility study. Radiology 2003;226:897–905.
54. McDannold N, Tempany CM, Fennessy FM, So MJ, Rybicki FJ, Stewart EA, et al. Uterine leiomyomas: MR imaging-based thermometry and thermal dosimetry during focused ultrasound thermal ablation. Radiology 2006;240:263–272.
55. He H-y, Lu L-l, Zhou Y-j, Nie Y-q., @ Clinical of study on curing leiomyoma with high intensity focused ultrasound. China J Modern Med 14, 37–41. 1–1–2004.
56. Gelet A, Chapelon JY, Margonari J, Theilliere Y, Gorry F, Souchon R, et al. High-intensity focused ultrasound experimentation on human benign prostatic hypertrophy. Eur Urol 1993;23:44–47.
57. Madersbacher S, Kratzik C, Susani M, Marberger M. Tissue ablation in benign prostatic hyperplasia with high intensity focused ultrasound. J Urol 1994;152:1956–1961.
58. Madersbacher S, Pedevilla M, Vingers L, Susani M, Marberger M. Effect of high intensity focused ultrasound on human prostate cancer in-vivo. Cancer Res 1995;55: 3346–3351.
59. Mulligan ED, Lynch TH, Mulvin D, Greene D, Smith JM, Fitzpatrick JM. High-intensity focused ultrasound in the treatment of benign prostatic hyperplasia. Br J Urol 1997;79:177–180.
60. Sanghvi NT, Fry FJ, Bihrle R, Foster RS, Phillips MH, Syrus J, Zaitsev AV, Hennige CW. Noninvasive surgery of prostate tissue by high-intensity focused ultrasound. IEEE Trans Ultrason Ferr 1996;43:1099–1110.
61. Sullivan LD, McLoughlin MG, Goldenberg LG, Gleave ME, Marich KW. Early experience with high-intensity focused ultrasound for the treatment of benign prostatic hypertrophy. Br J Urol 1997;79:172–176.
62. Madersbacher S, Schatzl G, Djavan B, Stulnig T, Marberger M. Long-term outcome of transrectal high- intensity focused ultrasound therapy for benign prostatic hyperplasia. Eur Urol 2000;37:687–694.
63. Chapelon JY, Gelet A, Souchon R, Pangaud C, Blanc E. Therapy using ultrasound: Application to localised prostate cancer. J D'Echographie et de Medecine Par Ultrasons 1998;19:260–264.
64. Gelet A, Chapelon JY, Bouvier R, Souchon R, Pangaud C, Abdelrahim AF, Cathignol D, Dubernard JM. Treatment of prostate cancer with transrectal focused ultrasound: Early clinical experience. Eur Urol 1996;29:174–183.
65. Gelet A, Chapelon JY, Bouvier R, Rouviere O, Lasne Y, Lyonnet D, Dubernard JM. Transrectal high-intensity focused ultrasound: Minimally invasive therapy of localized prostate cancer. J Endourol 2000;14:519–528.
66. Gelet A, Chapelon JY, Bouvier R, Rouviere O, Lyonnet D, Dubernard JM. Transrectal high intensity focused ultrasound for the treatment of localized prostate cancer: Factors influencing the outcome. Eur Urol 2001;40:124–129.
67. Madersbacher S, Marberger M. High-energy shockwaves and extracorporeal high-intensity focused ultrasound. J Endourol 2003;17:667–672.
68. Beerlage HP, Thuroff S, Debruyne FMJ, Chaussy C, de la Rosette JJMC. Transrectal high-intensity focused ultrasound using the ablatherm device in the treatment of localized prostate carcinoma. Urology 1999;54:273–277.

69. Beerlage HP, van Leenders GJLH, Oosterhof GON, Witjes JA, Ruijter ET, van de Kaa CA, Debruyne FMJ. High-intensity focused ultrasound (HIFU) followed after one to two weeks by radical retropubic prostatectomy: Results of a prospective study. Prostate 1999;39:41–46.
70. Chaussy C, Thuroff S. High-intensity focused ultrasound in prostate cancer: Results after 3 years. Mol Urol 2000;4:179–182.
71. Chaussy C, Thuroff S, dela Rosette JJMC. Results and side effects of high-intensity focused ultrasound in localized prostate cancer. J Endourol 2001;15:437–440.
72. Chaussy C, Thuroff S. The status of high-intensity focused ultrasound in the treatment of localized prostate cancer and the impact of a combined resection. Curr Urol Rep 2003;4:248–252.
73. Blana A, Walter B, Rogenhofer S, Wieland WF. High-intensity focused ultrasound for the treatment of localized prostate cancer: 5-year experience. Urology 2004;63: 297–300.
74. Poissonnier L, Gelet A, Chapelon JY, Bouvier R, Rouviere O, Pangaud C, et al. Results of transrectal focused ultrasound for the treatment of localized prostate cancer (120 patients with PSA < or + 10 ng/ml). Prog Urol 2003;13:60–72.
75. Blana A, Rogenhofer S, Ganzer R, Wild PJ, Wieland WF, Walter B. Morbidity associated with repeated transrectal high-intensity focused ultrasound treatment of localized prostate cancer. World J Urol 2006:585–590.
76. Poissonnier L, Chapelon JY, Rouviere O, Curiel L, Bouvier R, Martin X, et al. Control of prostate cancer by transrectal HIFU in 227 Patients. Eur Urol 2006;00.
77. Azzouz H, de la Rosette JJMC. HIFU: Local treatment of prostate cancer. EAU-EBU Update Series 2006;4:62–70.
78. Chaussy C, roff S, Rebillard X, Gelet A. Technology insight: High-intensity focused ultrasound for urologic cancers. Nat Clin Pract Urol 2005;2:191–198.
79. Gelet A, Chapelon JY, Poissonnier L, Bouvier R, Rouviere O, Curiel L, et al. Local recurrence of prostate cancer after external beam radiotherapy: Early experience of salvage therapy using high-intensity focused ultrasonography. Urology 2004;63:625–629.
80. Chaussy C, Thuroff S, Bergsdorf T. [Local recurrence of prostate cancer after curative therapy: HIFU (Ablatherm((R))) as a treatment option.]. Urologe A 2006;45:1271–1275.
81. Kratzik C, Schatzl G, Lackner J, Marberger M. Transcutaneous high-intensity focused ultrasonography can cure testicular cancer in solitary testis. Urology 2006;67: 1269–1273.
82. Bamber J, ter Haar GR, Hill C. Physical Principles of medical Ultrasound. 2nd ed. London: Wiley; 2004.
83. Hill CR. Optimum Acoustic Frequency for focused ultrasound surgery. Ultrasound Med Biol 1994;20:271–277.
84. Hynynen K, Watmough DJ, Mallard JR. The effects of some physical factors on the production of hyperthermia by ultrasound in neoplastic tissues. Radiat Environ Biophys 1981;19:215–226.
85. Duck F.A. Physical Properties of tissues: A comprehensive reference book. London: Academic Press; 1990.
86. Goss SA, Johnston RL, Dunn F. Comprehensive compilation of empirical ultrasonic properties of mammalian tissues. J Acoust Soc Am 1978;64:423–457.
87. Goss SA, Johnston RL, Dunn F. Compilation of empirical ultrasonic properties of mammalian tissues. II. J Acoust Soc Am 1980;68:93–108.
88. Clarke RL, Bush NL, ter Haar GR. The changes in acoustic attenuation due to in vitro heating. Ultrasound Med Biol 2003;29:127–135.
89. Zderic V, Keshavarzi A, Andrew MA, Vaezy S, Martin RW. Attenuation of porcine tissues in vivo after high-intensity ultrasound treatment. Ultrasound Med Biol 2004;30:61–66.
90. Browne JE, Ramnarine KV, Watson AJ, Hoskins PR. Assessment of the acoustic properties of common tissue-mimicking test phantoms. Ultrasound Med Biol 2003; 29:1053–1060.
91. Burlew MM, Madsen EL, Zagzebski JA, Banjavic RA, Sum SW. A new ultrasound tissue-equivalent material. Radiology 1980;134:517–520.
92. Lafon C, Zderic V, Noble ML, Yuen JC, Kaczkowski PJ, Sapozhnikov OA, Chavrier F, Crum L, Vaezy S. Gel phantom for use in high-intensity focused ultrasound dosimetry. Ultrasound Med Biol 2005;31:1383–1389.
93. Takegami K, Kaneko Y, Watanabe T, Maruyama T, Matsumoto Y, Nagawa H. Polyacrylamide gel containing egg white as new model for irradiation experiments using focused ultrasound. Ultrasound Med Biol 2004;30: 1419–1422.
94. Chen L, ter Haar GR, Hill CR, Dworkin M, Carnochan P, Young H, Bensted JPM. Effect of blood perfusion on the ablation of liver parenchyma with high-intensity focused ultrasound. Phys Med Biol 1993;38:1661–1673.
95. Huang J, Holt RG, Cleveland RO, Roy RA. Experimental validation of a tractable numerical model for focused ultrasound heating in flow-through tissue phantoms. J Acoust Soc Am 2004;116:2451–2458.
96. Pennes HH. Analysis of tissue and arterial blood temperatures in the resting human forearm. J Appl Phycol 1948;1:93–122.
97. Hamilton M.F, Blackstock DT. Nonlinear Acoustics. New York: Academic Press; 1998.
98. Leighton T.G. The Acoustic Bubble. London: Academic Press; 1994.
99. Coussios CC, Farny CH, ter Haar GR, Roy RA. Role of acoustic cavitation in the delivery and monitoring of cancer treatment by high-intensity focussed ultrasound. Int J Hyperther 2007, this issue.
100. Holt RG, Roy RA. Measurements of bubble-enhanced heating from focused, MHz-frequency ultrasound in a tissue-mimicking material. Ultrasound Med Biol 2001;27:1399–1412.
101. Hynynen K. The threshold for thermally significant cavitation in dog's thigh muscle in vivo. Ultrasound Med Biol 1991;17:157–169.
102. Khokhlova VA, Bailey MR, Reed JA, Cunitz BW, Kaczkowski PJ, Crum LA. Effects of nonlinear propagation, cavitation, and boiling in lesion formation by high intensity focused ultrasound in a gel phantom. J Acoust Soc Am 2006;119:1834–1848.
103. Melodelima D, Chapelon JY, Theillere Y, Cathignol D. Combination of thermal and cavitation effects to generate deep lesions with an endocavitary applicator using a plane transducer: Ex vivo studies. Ultrasound Med Biol 2004;30:103–111.
104. Bailey MR, Couret LN, Sapozhnikov OA, Khokhlova VA, ter Haar G, Vaezy S, Shi X, Martin R, Crum L. Use of overpressure to assess the role of bubbles in focused ultrasound lesion shape in vitro. Ultrasound Med Biol 2001;27:695–708.
105. Rabkin BA, Zderic V, Vaezy S. Hyperecho in ultrasound images of HIFU therapy: Involvement of cavitation. Ultrasound Med Biol 2005;31:947–956.
106. Yang X, Roy RA, Holt RG. Bubble dynamics and size distributions during focused ultrasound insonation. J Acoust Soc Am 2004;116:3423–3431.
107. Lunt MJ, Ashley B. A simple radiation balance for measuring ultrasonic power. J Med Eng Technol 1979;3:194–197.

108. Preston RC, Ed. Output Measurement for Medical Ultrasound. London: Springer-Verlag, 1991.
109. Shaw A. Delivering the right dose. Conference series: Advanced metrology for ultrasound in medicine. J Phys 2004;1:174–179.
110. Lewin PA, Bautista R, Devaraju V. Voltage sensitivity response of ultrasonic hydrophones in the frequency range 0.25–2.5 MHz. Ultrasound Med Biol 1999;25: 1131–1137.
111. Lewin PA, Barrie-Smith N, Ide M, Hynynen K, Macdonald M. Interlaboratory acoustic power measurement. J Ultrasound Med 2003;22:207–213.
112. Lewin PA, Mu C, Umchid S, Daryoush A, El Sherif M. Acousto-optic, point receiver hydrophone probe for operation up to 100 MHz. Ultrasonics 2005;43:815–821.
113. Lunt MJ, Ashley B. A simple radiation balance for measuring ultrasonic power. J Med Eng Technol 1979;3:194–197.
114. Schafer ME. Cost-effective shock wave hydrophones. J Stone Dis 1993;5:73–76.
115. Shotton KC, Bacon DR, Quilliam RM. A pvdf membrane hydrophone for operation in the range 0.5 Mhz to 15 Mhz. Ultrasonics 1980;18:123–126.
116. Hill CR, Rivens IH, Vaughan MG, ter Haar GR. Lesion development in focused ultrasound surgery: A general model. Ultrasound Med Biol 1994;20:259–269.
117. Hill CR, Rivens IH, Vaughan MG, ter Haar GR. Lesion development in focused ultrasound surgery: A general model. Ultrasound Med Biol 1994;20:259–269.
118. Sapareto SA, Dewey WC. Thermal dose determination in cancer therapy. Int J Radiat Oncol Biol Phys 1984;10:787–800.
119. Rivens I, Shaw A, Civale J, Morris M. Treatment Monitoring & Thermometryfor Therapeutic Focused Ultrasound. Int J Hyperther 2007, this issue.
120. Vaezy S, Zderic V. Haemorrhage control using high intensity focused ultrasound. Int J Hyperther 2007.
121. Fry FJ. Precision high intensity focused ultrasonic machines for surgery. Am J Phys Med 1958;37:152–156.
122. Chapelon JY, Cathignol D, Cain C, Ebbini E, Kluiwstra JU, Sapozhnikov OA, Fleury G, Berriet R, Chupin L, Guey JL. New piezoelectric transducers for therapeutic ultrasound. Ultrasound Med Biol 2000;26:153–159.
123. Clarke RL. Modification of intensity distributions from large aperture ultrasound sources. Ultrasound Med Biol 1995;21:353–363.
124. Cline HE, Hynynen K, Watkins RD, Adams WJ, Schenck JF, Ettinger RH, Freund WR, Vetro JP, Jolesz FA. Focused US system for MR imaging—guided tumour ablation. Radiology 1995;194:731–737.
125. Daum DR, Smith NB, King R, Hynynen K. In vivo demonstration of noninvasive thermal surgery of the liver and kidney using an ultrasonic phased array. Ultrasound Med Biol 1999;25:1087–1098.
126. Dupenloup F, Chapelon JY, Cathignol DJ, Sapozhnikov OA. Reduction of the grating lobes of annular arrays used in focused ultrasound surgery. IEEE Trans Ultrason Ferroelectr Freq Cont 1996;43:991–998.
127. Fjield T, Silcox CE, Hynynen K. Low-profile lenses for ultrasound surgery. Phys Med Biol 1999;44:1803–1813.
128. Goss SA, Frizzell LA, Kouzmanoff JT, Barich JM, Yang JM. Sparse random ultrasound phased-array for focal surgery. IEEE Transactions on Ultrason Ferroelectr Freq Cont 1996;43:1111–1121.
129. Hacker A, Chauhan S, Peters K, Hildenbrand R, Marlinghaus E, Alken P, Michel MS. Multiple high-intensity focused ultrasound probes for kidney-tissue ablation. J Endourol 2005;19:1036–1040.
130. Held R, Nguyen TN, Vaezy S. Transvaginal 3D image-guided high intensity focused ultrasound array. Applied Physics Laboratory, University of Washington, Seattle, WA, United States: Kyoto: 2005.
131. Hynynen K, Chung A, Fjield T, Buchanan M, Daum D, Colucci V, et al. Feasibility of using ultrasound phased-arrays for MRI monitored noninvasive surgery. IEEE Trans Ultrason Ferroelectr Freq Cont 1996;43:1043–1053.
132. Kohrmann KU, Michel MS, Steidler A, Marlinghaus E, Kraut O, Alken P. Technical characterization of an ultrasound source for noninvasive thermoablation by high-intensity focused ultrasound. BJU Int 2002;90:248–252.
133. Sasaki K, Azuma T, Kawabata KI, Shimoda M, Kokue EI, Umemura SI. Effect of split-focus approach on producing larger coagulation in swine liver. Ultrasound Med Biol 2003;29:591–599.
134. Wan H, Vanbaren P, Ebbini ES, Cain CA. Ultrasound surgery – comparison of strategies using phased-array systems. IEEE Trans Ultrason Ferroelectr Freq Cont 1996;43:1085–1098.
135. Wharton I, Rivens I, ter Haar G, Gilderdale D, Collins D, Hand J, Abel P, deSouza N. Design and development of a prototype endocavitary probe for high intensity focused ultrasound delivery with magnetic resonance imaging thermometry and guidance. JMRI 2007, in press.
136. Miller NR, Bamber JC, ter Haar GR. Imaging of temperature-induced echo strain: Preliminary in vitro study to assess feasibility for guiding focused ultrasound surgery. Ultrasound Med Biol 2004;30:345–356.
137. Miller NR, Bamber JC, Meaney PM. Fundamental limitations of noninvasive temperature imaging by means of ultrasound echo strain estimation. Ultrasound Med Biol 2002;28:1319–1333.
138. Miller NR, Bograchev KM, Bamber JC. Ultrasonic temperature imaging for guiding focused ultrasound surgery: Effect of angle between imaging beam and therapy beam. Ultrasound Med Biol 2005;31:401–413.
139. Anand A, Kaczkowski PJ. Monitoring formation of high intensity focused ultrasound (HIFU) induced lesions using backscattered ultrasound. Acoustic Research Letters Online 2004;5:88–94.
140. Andreou C, Blana A, Orovan W, Hassouna M, Warner J, Woods E. Technical review: High-intensity focused ultrasound for prostate cancer. Can J Urol 2005;12:2684–2685.
141. Christopher T. HIFU focusing efficiency and a twin annular array source for prostate treatment. IEEE Trans Ultrason Ferroelectr Freq Control 2005;52:1523–1533.
142. Curiel L, Chavrier F, Souchon R, Birer A, Chapelon JY. 1.5-D high intensity focused ultrasound array for non-invasive prostate cancer surgery. IEEE Trans Ultrason Ferroelectr Freq Control 2002;49:231–242.
143. Rebillard X, Gelet A, Davin JL, Soulie M, Prapotnich D, Cathelineau X, et al. Transrectal high-intensity focused ultrasound in the treatment of localized prostate cancer. J Endourol 2005;19:693–701.
144. Saleh KY, Smith NB. A 63 element 1.75 dimensional ultrasound phased array for the treatment of benign prostatic hyperplasia. Biomed Eng Online 2005;4:39.
145. Seip R, Chen W, Carlson R, Frizzell L, Buffet C, Cathignol D. Annular and cylindrical phased array geometries for transrectal High-Intensity Focused Ultrasound (HIFU) using PZT and piezocomposite materials.Proc ISTU4 AIP 2004;229–232.
146. Lafon C, Chapelon JY, Prat F, Gorry F, Margonari J, Theillere Y, Cathignol D. Design and preliminary results of an ultrasound applicator for interstitial thermal coagulation. Ultrasound Med Biol 1998;24:113–122.

147. Prat F, Lafon C, Margonari J, Gorry F, Theillere Y, Chapelon JY, Cathignol D. A high-intensity US probe designed for intraductal tumor destruction: Experimental results. Gastrointest Endosc 1999;50:388–392.
148. Prat F, Lafon C, Melodelima D, Theillere J-Y, Fritsch J, Pelletier G, Buffet C, Cathignol D. Endoscopic treatment of cholangiocarcinoma and carcinoma of the duodenal papilla by intraductal high-intensity US: Results of a pilot study. Gastrointest Endosc 2002;56:909–915.
149. Prat F, Lafon C, Theillere J-Y, Fritsch J, Choury A-D, Lorand I, Cathignol D. Destruction of bile duct carcinoma by intraductal high intensity ultrasound during ERCP. Gastrointest Endosc 2001;53:797–800.
150. Melodelima D, Salomir R, Mougenot C, Moonen C, Cathignon D. In vivo experiments with intraluminal ultrasound applicator compatible with ''real-time'' MR temperature mapping, designed for oesophagus tumour ablation. 2005;Proc ISTU4 AIP 185–187.
151. Melodelima D, Salomir R, Chapelon JY, re Y, Moonen C, Cathignol D. Intraluminal high intensity ultrasound treatment in the esophagus under fast MR temperature mapping: In vivo studies. Magn Reson Med 2005;54:975–982.
152. Makin I, Faikin W, Mast D, Runk M, Slayton M, Barthe P Conformal bulk ablation and therapy monitoring using intracorporeal image-Treat Ultrasound Arrays. Proc ISTU4AIP 2005;27–29.
153. Murat F, Lafon C, Gelet A, Martin X, Cathignol D Bloodless partial nephrectomy through application of non-focused high-intensity ultrasound. Proc ISTU4 AIP 2005;181–184.
154. Wu F, Wang ZB, Chen WZ, Zou JZ, Bai J, Zhu H, Li JQ, Jin CB, Xie FL, Su HB. Advanced hepatocellular carcinoma: Treatment with high-intensity focused ultrasound ablation combined with transcatheter arterial embolization. Radiology 2005;235:659–667.
155. Illing RO, Kennedy JE, Wu F, ter Haar GR, Protheroe AS, Friend PJ, Gleeson FV, Cranston DW, Phillips RR, Middleton MR. The safety and feasibility of extracorporeal high-intensity focused ultrasound (HIFU) for the treatment of liver and kidney tumours in a Western population. Br J Cancer 2005;93:890–895.
156. Wu F, Wang ZB, Zhu H, Chen WZ, Zou JZ, Bai J, Li JQ, Jin CB, Xie FL, Su HB. Extracorporeal high intensity focused ultrasound treatment for patients with breast cancer. Breast Cancer Res Treat 2005;92:51–60.
157. Chen W, Wang Z, Wu F, Zhu H, Zou J, Bai J, Li JQ, Xie FL. High intensity focused ultrasound in the treatment of primary malignant bone tumor. Zhonghua Zhong Liu Za Zhi 2002;24:612–615.
158. Wu F, Wang ZB, Zhu H, Chen WZ, Zou JZ, Bai J, Li JQ, Jin CB, Xie FL, Su HB. Feasibility of US-guided high-intensity focused ultrasound treatment in patients with advanced pancreatic cancer: Initial experience. Radiology 2005;236:1034–1040.
159. Sanghvi NT, Foster RS, Bihrle R, Casey R, Uchida T, Phillips MH, Syrus J, Zaitsev AV, Marich WN, Fry FJ. Noninvasive surgery of prostate tissue by high intensity focused ultrasound: An updated report. Eur J Ultrasound 1999;9:19–29.
160. High-Intensity Focused Ultrasound (HIFU) for the treatment of localized prostate cancer using sonablate-500. 04 Sep 18; Department of Urology, Tokai University Hachioji Hospital, Hachioji, Japan: Kyoto; 2005.
161. Li C, Bian D, Chen W, Zhao C, Yin N, Wang Z. Focused ultrasound therapy of vulvar dystrophies: A feasibility study. Obstet Gynecol 2004;104:915–921.
162. Thomas R, Farny CH, Coussios CC, Roy RR, Holt RG. Dynamics and control of cavitation during high-intensity focused ultrasound application. Acoust Res Lett Onl 2005;6:182–187.